Synthesis, Structure, and Characterization of a Phenolate-Bridged Dimanganese(II) Complex of a Dinucleating Phenol Ligand

Yilma Gultneh,* Amjad Farooq, Shuncheng Liu, Kenneth D. Karlin,† and Jon Zubieta‡

Departments of Chemistry, Howard University, Washington, D.C. 20059, The Johns Hopkins University, Baltimore, Maryland 21218, and Syracuse University, Syracuse, New York 13244

Received January 24, 1992

The dinucleating phenol ligand LOH (LOH = 2,6-bis((bis(2-(2-pyridyl)ethyl)amino)methyl)phenol (**1**)) is reacted with $Mn(ClO_4)_2 \cdot 6H_2O$ in the presence of excess acetate anion and a base (NEt_3) in methanol to produce the dinuclear Mn^{II}_2 complex $[Mn_2(LO)(OAc)_2]ClO_4$ (**5**) which crystallizes in the monoclinic space group $P2_1/n$ with unit cell dimensions a = 11.227 (3) Å, b = 21.815 (8) Å, c = 17.731 (7) Å, α = 90.00 (3)°, β = 102.45 (3)°, and γ = 90.00 (3)°, with four molecules per unit cell. The structure shows that two acetate anions and a phenoxy oxygen bridge the manganese ions. The $[Mn_2(LO)(\mu\text{-}OAc)_2]^+$ cation has a noncrystallographic C_2 axis with the two Mn(II) ions in a nearly equivalent distorted octahedron coordination environment. Cyclic voltammetry of **5** in acetonitrile shows a reversible peak at 0.73 V and an irreversible peak at 1.28 V (vs Ag/AgCl). The two redox potentials assigned to the $Mn^{II}_2/Mn^{II}Mn^{III}$ and the $Mn^{II}Mn^{III}/Mn^{III}_2$ redox processes are significantly higher than the potentials assigned to the same processes in the analogous but mixed-valent $Mn^{II}Mn^{III}$ complexes showing that ligand **1** stabilizes the lower oxidation states. This is attributed to the six-membered chelate rings in **5** vs five-membered rings found in the mixed-valent complexes. Complex **5** is the first example of a structurally characterized stable discrete dinuclear Mn^{II}_2 complex in this series of analogous complexes. The EPR spectrum of the crystals of **5** at 77 K shows six peaks with no hyperfine structures whereas in DMF/methanol frozen glass it shows a set of six peaks centered near g = 2 with an 11-line hyperfine structure (J = 43 G) superimposed and observable on the two lower field peaks. The hyperfine structure is attributed to the isotropic coupling to the nuclei of the two equivalent Mn(II) ions (total nuclear spin I = 5). A peak for the ΔM_s = 2 forbidden transition at half-field and two outer flanking peaks are also observed. A superimposed six-peak hyperfine structure observed at g = 2 (J = 80 G) is due to impurity caused by monomeric Mn(II) species.

Introduction

The active sites of the redox-active manganese enzymes such as the photosynthetic water-oxidizing enzyme photosystem II (PS II),[1] manganese catalase,[2a-d] and ribonucleotide reductase[2e,f] in certain bacteria are believed to have dinuclear or tetranuclear centers. In PS II, where there are four manganese ions per enzyme molecule, the EPR spectrum in the S_2 state shows evidence that at least two manganese ions are magnetically coupled.[3] Other models including trinuclear and tetranuclear complexes and a dimer of dinuclear active centers have also been suggested to explain the EPR and EXAFS data.[4] These findings have prompted interest in the studies of synthetic dinuclear[5] and tetranuclear manganese complexes of biologically relevant N and O donor ligands with oxo, phenoxo, and alkoxo bridging and in many cases with additional carboxylate bridges. The series of dinucleating phenolic ligands bpmp (**2**), HL-Im (**3**), and bcmp (**4**) in which the phenoxy oxygen acts as a bridge between metal ions, have been shown to yield the phenoxo- and acetato-bridged mixed-valent $Mn^{II}Mn^{III}$ complexes $[Mn_2(bpmp)(\mu\text{-}(OAc)_2]^{2+}$

* To whom correspondence should be addressed at Howard University.
† Johns Hopkins University.
‡ Syracuse University.

(1) (a) Dismukes, G. C. *Photochem. Photobiol.* **1986**, *43*, 99–115. Pecararo, V. L. *Photochem. Photobiol.* **1988**, *49*, 249. (b) Renger, G. *Angew. Chem. Int. Ed. Engl.* **1987**, *26*, 643–660. (c) Dismukes, G. C.; Siderer, Y. *FEBS Lett.*, **1980**, *212*, 78–80. (d) Hansson, O. R.; Aosa, R.; Vangard, T. *Biophys. J.* **1987**, *51*, 825. (e) Prince, R. C. *Trends Biochem. Sci.* **1987**, *894*, 91. (f) Brudvig, G. W. *J. Bioenerg. Biomembr.* **1987**, *19*, 91. (g) Brudwig, G. W. In *Metal Clusters in Proteins*, Que, L., Ed., ACS Symposium Series 372; American Chemical Society: Washington, DC, 1988; pp 221–237. (h) Amesz, J. Biochim. *Biophys. Acta* **1983**, *726*, 1. (i) Dismukes, G. C.; Ferris, K.; Watnik, P. *Photochem. Photobiol.* **1982**, *3*, 243. (j) Penner-Hahn, J. E.; Fronko, R. M.; Pecoraro, V. L.; Yokum, C. F.; Betts, S. D.; Bowlby, N. R. *J. Am. Chem. Soc.* **1990**, *112*, 2549–2557. (k) Kuwabara, T.; Miyao, M.; Murata, N.; Murata, T. *Biochim. Biophys. Acta* **1985**, *806*, 283–289. (l) Brudvig, G. W.; Beck, W. F.; DePaula, J. C. *Annu. Rev. Biophys. Biophys. Chem.* **1989**, *18*, 25–46.

(2) (a) Renger, G.; Weiss, W. *Biochem. Biophys. Acta* **1986**, *850*, 184. (b) Brudvig, G. W.; Crabtree, R. H. *Proc. Natl. Acad. Sci. U.S.A.* **1986**, *83*, 4586. (c) Kumabara, T.; Govindjee. *Proc. Natl. Acad. Sci. U.S.A.* **1985**, *82*, 6119. (d) Beyer, W. F.; Fridovich, I. *Biochemistry* **1985**, *24*, 6460–6467. (e) Plonzig, J.; Auling, G. *Arch. Microbiol.* **1987**, *146*, 396–401. (f) Willing, A.; Follman, H.; Auling, G. *Eur. J. Biochem.*, **1988**, *170*, 603–611.

(3) (a) Kuwabara, T.; Miyao, M.; Murata, N.; Murata, T. *Biochim. Biophys. Acta* **1985**, *806*, 283–289. (b) Dismukes, G. C. *Photochem. Photobiol.* **1986**, *43*, 99–115.

(4) (a) Kim, D. H.; Britt, R. D.; Klein, M. P.; Sauer, K. J. *J. Am. Chem. Soc.* **1990**, *112*, 9389. (b) George, G. N.; Prince, R. C.; Cramer, S. C. *Science* **1989**, *243*, 789–791. (c) DePaula, J. C.; Beck, W. F.; Brudvig, G. W.; *J. Am. Chem. Soc.* **1986**, *108*, 4002. (d) DePaula, J. C.; Beck, W. F.; Miller, A-F., Wilson, R. B.; Brudwig, W. *J. Chem. Soc., Faraday Trans. 1*, **1987**, *83*, 3636–3651. (e) Brudwig, G. W. In *Advanced EPR Applications in Biochemistry*, Hoff, A. J.; Ed.; Elsevier: Amsterdam, 1989; pp 839–863. (f) Giles, R. D.; Yachandra, V. K.; McDermott, A. E.; DeRose, V. J.; Zimmermann, J.-L.; Sauer, K.; Klein, M. P. In *Current Research in Photosynthesis*; Battscheffsky, M., Ed.; Kluwer Academic Publishers: Dordrecht, The Netherlands, 1991. *J. Am. Chem. Soc.* **1991**, *113*, 5055–5057.

(5) (a) Brewer, K. J.; Calvin, M.; Lumpkin, R. S.; Otvos, J. W.; Spreer, L. O. *Inorg. Chem.*, **1989**, *28*, 4446–4451. (b) Cooper, S. R.; Dismukes, G. C.; Klein, M. P.; Calvin, M. *J. Am. Chem. Soc.* **1978**, *100*, 7248–7252. (c) Plaskin, P. M.; Stoufer, R. C.; Mathew, M.; Palenik, G. J. *J. Am. Chem. Soc.* **1972**, *94*, 2121–2122. (d) Collins, M. A.; Hodgson, D. J.; Michelsen, K.; Towle, D. K. *J. Chem. Soc., Chem. Commun.* **1987**, 1659–1660. (e) Towle, D. K.; Botsford, C. A.; Hodgson, D. J. *Inorg. Chim. Acta* **1988**, *141*, 167–168. (f) Hagen, K. S.; Armstrong, W. H.; Hope, H. *Inorg. Chem.* **1988**, *27*, 967–969. (g) Mikuriya, M.; Torihara, N.; Okawa, H.; Kida, S. *Bull. Chem. Soc. Jpn.* **1981**, *54*, 1063–1067. (h) Que, L., Jr.; True, A. E. In *Progress in Inorganic Chemistry*; Lippard, S. J., Ed.; Wiley: New York, 1990; Vol. 38, pp 97–200.

(6) (a) Vincent, J. B.; Christmas, C.; Chang, H.-R.; Qiaoying, L.; Boyd, P. D. W.; Huffman, J. C.; Hendrickson, D. N.; Christou, G., *J. Am. Chem. Soc.* **1989**, *111*, 2086–2097. (b) Vincent, J. B.; Christmas, C.; Huffman, J. C.; Christou, G.; Chang, H.-R.; Hendrickson, D. N. *J. Chem. Soc., Chem. Commun.* **1987**, 1303.

0020-1669/92/1331-3607$03.00/0

(**6**),[7] $[Mn_2(L\text{-}Im)(\mu\text{-}OAc)_2]^{2+}$ (**7**),[8] and $[Mn_2(bcmp)(\mu\text{-}OAc)_2]^{2+}$ (**8**),[9a] respectively. These have been structurally characterized and their magnetic, electronic, and electrochemical properties have been reported.

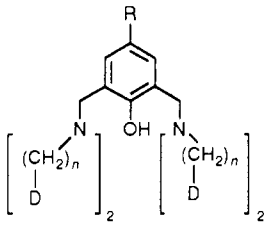

	R	*n*	D
1 (LOH)	H	2	2-pyridyl
2 (bpmp)	CH_3	1	2-pyridyl
3 (HL-Im)	CH_3	1	1-methylimidazol-2-yl
4 (bcmp)	CH_3	1	1,4,7-triazanon-1-yl

The dinucleating phenol ligand **1** is similar to **2–4**, but it provides a variation in this class of ligands in its coordination to metal ions. The presence of the longer chelate arms in **1** is expected to have consequences on the stabilities of the various oxidation states and thereby confer a different set of redox properties to the complex.

Here we report the synthesis, structure and properties of the dinuclear manganese complex of the ligand **1** (2,6-bis(((bis(2-(2-pyridyl)ethyl)amino)methyl)phenol) (LOH) which, unlike the above related ligands **2** and **3**, yields a stable dinuclear Mn^{II}_2 complex $[Mn_2(LO^-)(\mu\text{-}OAc)_2](ClO_4)$ (**5**). The structures of Mn^{II}_2 dinuclear complexes of macrocyclic Robson type ligands with acetates bridging dinuclear units and forming infinite chains have been reported;[9b] however, complex **5** is the first structurally characterized discrete Mn^{II}_2 dinuclear stable complex.[5h]

Experimental Section

Solvents were refluxed and distilled from drying agents under argon as follows: methanol from magnesium methoxide, CH_3CN and DMF from CaH_2, and diethyl ether from sodium/benzophenone. Other reagents were used as received.

Measurements. Elemental analysis was performed by Galbraith Laboratories, Inc. Knoxville, TN. Infrared spectra were taken on a Perkin-Elmer 710 B spectrophotometer, and ^1H NMR spectra were recorded on a 300-MHz Varian XL-300 spectrometer. Room-temperature magnetic susceptibility of the powdered sample was measured using a Johnson Matthey magnetic susceptibility balance. The Evans method[10] was used to determine the magnetic susceptibility of **5** in solution. A 1:1 mixture of DMF and DMF-d_7 was used as solvent. A coaxial inner tube inside a 5-mm NMR sample tube contained pure DMF. The paramagnetic shift of the resonance peak of the methyl protons of DMF in the complex solution relative to those of the pure DMF was measured and used to calculate the magnetic susceptibility of the complex. X-Band EPR spectra of the crystalline sample and the frozen DMF/methanol (1:1 mixture) glass were taken at 77 K (liquid nitrogen temperature) using a Varian E-4 spectrometer with DPPH as standard. Cyclic voltammetry measurements were run on CH_3CN solutions which were 0.10 M in the complex and 0.20 M in $n\text{-}Bu_4NPF_6$ supporting electrolyte using a Bioanalytical Systems (BAS) CV-27 voltammograph at 25 °C. A glassy-carbon working electrode, a Ag/AgCl reference electrode (0.20 V vs NHE), and Pt auxiliary electrodes were employed. Molar conductivities of 1.0 mM solutions of the complex in DMF were determined using a Model PM-70 CB Barnstead conductivity bridge and a YSI Model 3403 conductivity cell.

Table I. Crystal Data for $[Mn_2(LO)(\mu\text{-}OAc)_2]ClO_4$ (**5**)

a, Å	11.227 (3)	chem formula	$C_{40}ClH_{45}Mn_2N_6O_9$
b, Å	21.815 (8)	fw	898.3
c, Å	17.731 (7)	r_{calcd}, g cm^{-3}	1.664
α, deg	90.00 (3)	temp, K	294
β, deg	102.45 (3)	λ, Å	0.710 73
γ, deg	90.00 (3)	no. of reflcns collcd	6118
V, Å^3	4240 (2)	no. of reflcns used in soln	4112
space group	$P2_1/n$		
Z	4	*R*	0.0757
		R_w	0.0780 04

Synthesis of the Ligand. The ligand **1** (LOH) was synthesized according to the literature method[11] in which α,α-bis(bis(2-(2-pyridyl)ethyl)amine)-*m*-xylene was first synthesized and purified followed by its hydroxylation at the 2-position of the *m*-xylene connecting the two bis(pyridylethyl)-amine arms by the reaction of its Cu(I) dinuclear complex with dioxygen. The hydroxylated ligand was isolated as the Cu(II) complex from which it was extracted by removing the Cu(II) ion using aqueous ammonia. After extraction of the ligand with CH_2Cl_2, the solution was dried over anhydrous $MgSO_4$, the solvent was removed by rotary evaporator, and the ligand was purified by flash column chromatography through a column of neutral alumina using an acetone/methanol (1:1) mixed solvent. The fractions collected were tested for purity by thin-layer chromatography on Baker-Flex 1B TLC plates in acetone solvent and by proton NMR.

Synthesis of the Complex $[Mn_2(LO)(\mu\text{-}OAc)_2]ClO_4$ (5) (LOH = 2,6-((Bis(2-(2-pyridyl)ethyl)amino)methyl)phenol). A methanol solution (50 mL) of the ligand (1.6 g, 2.8 mmol), triethylamine (0.31 g, 3.0 mmol), and sodium acetate (0.98 g, 12 mmol) was added to $Mn(ClO_4)_2\cdot 6H_2O$ (0.49 g, 6.0 mmol) dissolved in methanol (20 mL) and stirred under argon. In about 3–5 min, a colorless powdery precipitate formed. The mixture was allowed to stir overnight. The precipitate was filtered and redissolved in 50 mL of CH_2Cl_2 under argon, to this solution was added dry ether to the cloud point, and the mixture was allowed to stand overnight. The clear colorless crystals which formed were isolated and found to be suitable for X-ray diffraction crystallography. Anal. Calcd for $C_{40}H_{45}ClMn_2N_6O_5$: C, 53.40; H, 5.01; N, 9.35. Found: C, 53.20; H, 4.94; N, 9.04.

X-ray Crystallography: Data Collection, Reduction and Structure Solution, and Refinement. An epoxy-covered crystal of complex **5** was mounted on a Nicolet R3m four-circle automated diffractometer with a Mo X-ray source equipped with a highly ordered graphite monochromator (λ(Mo Kα) = 0.710 73 Å). Automatic centering and least-squares routines were carried out on 30 reflections to obtain the cell dimensions. The 2θ scan mode was employed for data collection. Three check reflections were measured every 197 reflections; these showed no significant decay during data collection. The program XTAPE of the SHELXTL package was used to process the data. Complex **5** crystallizes in the monoclinic space group $P2_1/n$ with $Z = 4$. The positional parameters of the Mn atoms were determined by the Patterson method. The remaining non-hydrogen atoms were located by subsequent difference Fourier maps and least-squares refinements. Atomic scattering factors for neutral atoms were used throughout the analysis. All atoms with the exception of hydrogen and carbon were refined anisotropically. Hydrogen atoms were included in the final stages of the refinement. The carbon–hydrogen bond lengths were set at 0.96 Å, and the thermal parameters were 1.2 times those of the bonded carbon atoms. The perchlorate anion for the complex was unexceptional, and no unusual bond distances or angles were observed. The final agreement *R* factor and refinement data along with a summary of unit cell parameters, data collection parameters, and refinement results are summarized in Table I. The final atomic coordinates and equivalent isotropic displacement parameters, along with their deviations, are shown in Table II. Selected bond lengths and bond angles are shown in Tables III and IV respectively. A full listing of atomic coordinates and equivalent isotropic displacement parameters (Table V), bond lengths (Table VI), and bond angles (Table VII) along with tables of anisotropic displacement parameters (Table VIII), hydrogen atom coordinates, and isotropic displacement parameters (Table IX) are available as supplementary material.

(7) (a) Diril, H.; Chang, H.-R.; Zhang, X.; Larasen, S. K.; Potenza, J. A.; Pierpont, C. G.; Schugar, H. J.; Isied, S. S.; Hendrickson, D. N. *J. Am. Chem. Soc.* **1987**, *109*, 6207–6208. (b) Christou, G.; Vincent, J. B. In *Metal Clusters in Proteins*; Que, L., Ed., ACS Symposium Series 372; American Chemical Society: Washington, DC, 1988; pp 238–255.

(8) Buchanan, R. M.; Oberhausen, K. J.; Richardson, J. F. *Inorg. Chem.* **1988**, *27*, 973–974.

(9) (a) Diril, H.; Chang, H.-R.; Nigles, M. J.; Zhang, X.; Potenza, J. A.; Schugar, H. J.; Isied, S. S.; Hendrickson, S. N. *J. Am. Chem. Soc.* **1989**, *111*, 5102–5114. (b) Luneau, D.; Savariault, J.-M.; Cassoux, P.; Tuchagues, J.-P. *J. Chem. Soc., Dalton Trans.* **1988**, 1225–1235.

(10) Evans, D. F.; *J. Chem. Soc.* **1959**, 2003–2005.

(11) Karlin, K. D.; Hayes, J. C.; Gultneh, Y.; Cruse, R. W.; McKown, J. W.; Hutchinson, J. P.; Zubieta, J. *J. Am. Chem. Soc.* **1984**, *106*, 2121–2128.

Table II. Atomic Coordinates (×10⁴) for $[Mn_2(LO)(OAc)_2](ClO_4)$ (**5**)

	x	*y*	*z*
Mn(1)	8602 (1)	3034 (1)	4116 (1)
Mn(2)	10432 (1)	1732 (1)	3866 (1)
O(1)	8900 (4)	2288 (2)	3412 (2)
O(2)	8915 (5)	2490 (2)	5126 (3)
O(3)	9745 (5)	1598 (2)	4918 (3)
O(4)	10487 (5)	3337 (2)	4279 (3)
O(5)	11573 (5)	2485 (2)	4275 (3)
C(1)	8021 (6)	1082 (3)	3137 (4)
C(2)	7680 (6)	1597 (3)	2559 (4)
C(3)	6845 (8)	1504 (4)	1852 (5)
C(4)	6533 (8)	1963 (4)	1329 (5)
C(5)	7031 (8)	2543 (4)	1494 (4)
C(6)	7825 (6)	2658 (3)	2191 (4)
C(7)	8156 (6)	2180 (3)	2741 (4)
C(8)	8363 (8)	3273 (3)	2383 (5)
N(1)	9332 (5)	893 (2)	3260 (3)
N(2)	11898 (6)	1034 (3)	4457 (4)
C(21)	12911 (8)	1302 (4)	4874 (5)
C(22)	13821 (8)	1000 (5)	5351 (5)
C(23)	13745 (9)	383 (5)	5409 (6)
C(24)	12741 (9)	90 (4)	4983 (5)
C(25)	11828 (8)	420 (3)	4515 (4)
C(26)	10740 (8)	89 (4)	4050 (4)
C(27)	9500 (7)	407 (3)	3866 (4)
N(3)	11014 (5)	1879 (3)	2679 (3)
C(31)	11114 (7)	2457 (4)	2458 (5)
C(32)	11138 (9)	2519 (4)	1714 (5)
C(33)	11006 (11)	2168 (5)	1158 (6)
C(34)	10927 (10)	1582 (4)	1382 (5)
C(35)	10935 (7)	1438 (4)	2145 (5)
C(36)	10849 (8)	792 (3)	2407 (5)
C(37)	9585 (7)	639 (3)	2534 (4)
N(4)	7905 (6)	3604 (3)	3006 (4)
N(5)	6532 (6)	2720 (3)	3935 (4)
C(51)	6352 (8)	2133 (5)	4096 (5)
C(52)	5252 (9)	1838 (6)	3849 (6)
C(53)	4334 (9)	2154 (7)	3442 (7)
C(54)	4477 (9)	2754 (7)	3260 (6)
C(55)	5597 (7)	3033 (5)	3515 (4)
C(56)	5815 (8)	3681 (5)	3339 (5)
C(57)	6559 (8)	3724 (4)	2716 (5)
N(6)	8413 (6)	3916 (3)	4807 (4)
C(61)	8545 (8)	3829 (4)	5573 (5)
C(62)	8619 (9)	4295 (5)	6068 (6)
C(63)	8615 (10)	4889 (6)	5802 (8)
C(64)	8504 (10)	4988 (5)	5057 (7)
C(65)	8397 (8)	4498 (4)	4552 (6)
C(66)	8214 (10)	4644 (4)	3713 (6)
C(67)	8594 (9)	4186 (3)	3159 (5)
C(68)	9245 (7)	1952 (4)	5313 (4)
C(69)	9026 (9)	1718 (4)	6061 (5)
C(70)	12617 (8)	3405 (4)	4591 (6)
C(71)	11467 (7)	3055 (3)	4368 (4)
Cl(1)	5850 (2)	604 (1)	7200 (1)
O(6)	6435 (9)	14 (4)	7167 (6)
O(7)	6704 (9)	823 (4)	6428 (4)
O(8)	6265 (11)	1019 (5)	7602 (6)
O(9)	8064 (8)	599 (4)	7508 (7)

Results and Discussion

The stoichiometry of the reaction for the synthesis of the complex $[Mn_2(LO)(OAc)_2](ClO_4)$ (**5**) is given by

$$2Mn(ClO_4)_2{\cdot}6H_2O + LOH + NEt_3 + 2CH_3COO^- \rightarrow [Mn_2(LO)(OOCCH_3)_2](ClO_4) + HNEt_3^+ + 3ClO_4^- + 6H_2O$$

5

The reaction requires the deprotonation of the phenol group of the ligand by NEt_3 and the presence of excess acetate ion in order to force the formation of the acetate complex in higher yield. When only a stoichiometric amount of sodium acetate is used, a second as yet undetermined product beside **5** is also obtained.

Table III. Principal Bond Lengths (Å) in $[Mn_2(LO)(OAc)_2](ClO_4)$ (**5**)

Mn(1)–O(1)	2.121 (5)	Mn(1)–O(2)	2.114 (5)
Mn(1)–O(4)	2.176 (6)	Mn(1)–N(4)	2.317 (6)
Mn(1)–N(5)	2.378 (7)	Mn(1)–N(6)	2.314 (7)
Mn(2)–O(1)	2.115 (4)	Mn(2)–O(3)	2.187 (6)
Mn(2)–O(5)	2.113 (5)	Mn(2)–N(1)	2.335 (5)
Mn(2)–N(2)	2.322 (6)	Mn(2)–N(3)	2.355 (7)
O(1)–C(7)	1.320 (7)	O(2)–C(68)	1.254 (9)
O(3)–C(68)	1.254 (10)	O(4)–C(71)	1.241 (10)
O(5)–C(71)	1.262 (9)	C(1)–C(2)	1.514 (10)
C(1)–N(1)	1.498 (9)	C(2)–C(3)	1.409 (10)
C(2)–C(7)	1.391 (10)	C(3)–C(4)	1.358 (12)
C(4)–C(5)	1.390 (13)	C(5)–C(6)	1.383 (9)
C(6)–C(7)	1.422 (10)	C(6)–C(8)	1.480 (10)
C(8)–N(4)	1.501 (11)	N(1)–C(27)	1.493 (9)
N(1)–C(37)	1.485 (9)	N(2)–C(21)	1.349 (10)
N(2)–C(25)	1.345 (10)	C(21)–C(22)	1.349 (12)

Table IV. Principal Bond Angles (deg) in $[Mn_2(LO)(OAc)_2](ClO_4)$ (**5**)

O(1)–Mn(1)–O(2)	92.7 (2)	O(1)–Mn(1)–O(4)	92.2 (2)
O(2)–Mn(1)–O(4)	94.5 (2)	O(1)–Mn(1)–N(4)	88.8 (2)
O(2)–Mn(1)–N(4)	170.1 (2)	O(4)–Mn(1)–N(4)	95.2 (2)
O(1)–Mn(1)–N(5)	88.5 (2)	O(2)–Mn(1)–N(5)	86.0 (2)
O(4)–Mn(1)–N(5)	179.1 (2)	N(4)–Mn(1)–N(5)	84.3 (2)
O(1)–Mn(1)–N(6)	173.4 (2)	O(2)–Mn(1)–N(6)	92.1 (2)
O(4)–Mn(1)–N(6)	82.8 (2)	N(4)–Mn(1)–N(6)	87.2 (2)
N(5)–Mn(1)–N(6)	96.4 (3)	O(1)–Mn(2)–O(3)	89.6 (2)
O(1)–Mn(2)–O(5)	93.9 (2)	O(3)–Mn(2)–O(5)	96.3 (2)
O(1)–Mn(2)–N(1)	88.2 (2)	O(3)–Mn(2)–N(1)	92.2 (2)
O(5)–Mn(2)–N(1)	171.3 (2)	O(1)–Mn(2)–N(2)	170.7 (2)
O(3)–Mn(2)–N(2)	82.6 (2)	O(5)–Mn(2)–N(2)	92.1 (2)
N(1)–Mn(2)–N(2)	86.9 (2)	O(1)–Mn(2)–N(3)	86.7 (2)
O(3)–Mn(2)–N(3)	175.6 (2)	O(5)–Mn(2)–N(3)	86.4 (2)
N(1)–Mn(2)–N(3)	85.3 (2)	N(2)–Mn(2)–N(3)	100.8 (2)
Mn(1)–O(1)–Mn(2)	115.8 (2)	Mn(1)–O(1)–C(7)	121.2 (4)
Mn(2)–O(1)–C(7)	123.0 (4)	Mn(1)–O(2)–C(68)	137.4 (5)
Mn(2)–O(3)–C(68)	132.6 (5)	Mn(1)–O(4)–C(71)	132.6 (5)
Mn(2)–O(5)–C(71)	138.0 (5)	C(2)–C(1)–N(1)	113.5 (6)
C(1)–C(2)–C(3)	121.2 (6)	C(1)–C(2)–C(7)	119.5 (6)
C(3)–C(2)–C(7)	119.2 (7)	C(2)–C(3)–C(4)	121.6 (8)
C(3)–C(4)–C(5)	119.8 (7)	C(4)–C(5)–C(6)	120.4 (7)
C(5)–C(6)–C(7)	120.2 (7)	C(5)–C(6)–C(8)	121.5 (7)
C(7)–C(6)–C(8)	118.3 (6)	O(1)–C(7)–C(2)	120.6 (6)
O(1)–C(7)–C(6)	120.6 (6)	C(2)–C(7)–C(6)	118.8 (6)
C(6)–C(8)–N(4)	114.7 (7)	Mn(2)–N(1)–C(1)	104.9 (4)
Mn(2)–N(1)–C(27)	104.7 (4)	C(1)–N(1)–C(27)	105.5 (6)
Mn(2)–N(1)–C(37)	120.7 (4)	C(1)–N(1)–C(37)	110.0 (5)
C(27)–N(1)–C(37)	109.9 (5)	Mn(2)–N(2)–C(21)	113.3 (5)
Mn(2)–N(2)–C(25)	129.8 (5)	C(21)–N(2)–C(25)	116.5 (7)

Structure of $[Mn_2(LO)(\mu\text{-}OAc)_2](ClO_4)$ (5). Crystal data and atomic coordinates are given in Tables I and II, respectively. Tables III and IV summarize the principal bond lengths and angles respectively. Figure 1 shows the ORTEP drawing of the cation $[Mn_2(LO)(\mu\text{-}OAc)_2]^+$. Complex **5** is a dinuclear complex with two crystallographically independent but nearly equivalent Mn^{2+} ions each in a slightly distorted octahedral coordination to three nitrogen and three oxygen donors. The Mn···Mn distance is 3.589 (3) Å. The phenoxy oxygen and two acetate groups bridge the two Mn^{2+} ions. The phenoxy oxygen is symmetrically bonded to the two Mn^{2+} ions whereas the two acetate groups are unsymmetrically bridging and slightly staggered relative to each other. This is shown by the unequal Mn–O distances of the two oxygens of each bridging acetate to the two manganese ions. One acetate forms a longer Mn–O distance to Mn(1) while the second acetate forms a longer Mn–O distance to Mn(2). The observed Mn–O and Mn–N bond lengths (Table III) are all in the ranges normally observed in Mn^{2+} complexes.[12] The Mn–N distances for pyridyl nitrogen atoms trans to the phenoxy oxygen are slightly

(12) (a) Shauer, C. K.; Anderson, P.; Eaton, G. R. *Inorg. Chem.* **1985**, *34*, 4082–4086. (b) Shannon, R. D. *Acta Crystallogr.* **1976**, *A32*, 751–767. Mabad, B.; Cassoux, P.; Tuchagues, J.-P.; Hendrickson, D. N. *Inorg. Chem.* **1986**, *25*, 1420–1431.

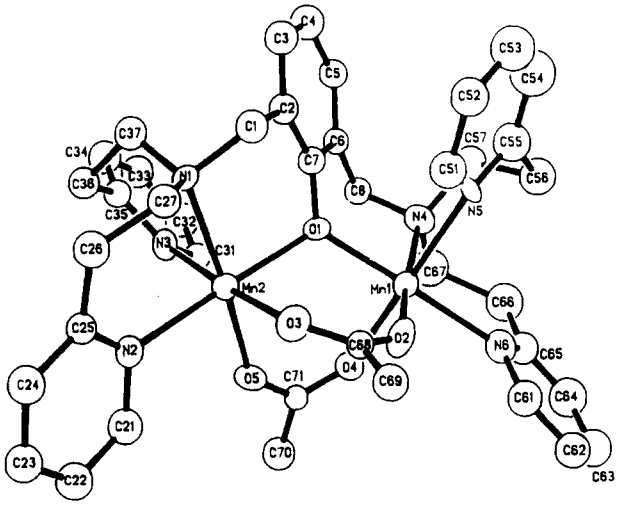

Figure 1. ORTEP diagram of the cationic portion of **5**, $[Mn_2(LO)(\mu\text{-}OAc)_2]^+$.

shorter than those for the cis pyridyl nitrogens. A comparison of the coordination distances of Mn(II) in **5** to those of Mn(II) in the valence-trapped mixed-valent $Mn^{II}Mn^{III}$ complexes **6** and **7** of ligands **2** and **3**, respectively, reveals some notable differences. Thus while Mn(II)–N_{amine} distances are closely similar in **5**–**7** the Mn–$N_{aromatic}$ distances in **5** (2.378, 2.322 Å) are longer than those in **6** (2.27, 2.21 Å) and in **7** (2.186, 2.229 Å). The Mn–$O_{phenoxy}$ distances in **5** (2.121, 2.115 Å) are shorter than the corresponding distances in **6** (2.193 Å) and in **7** (2.258 Å).[9] The Mn···Mn distance is longer in **5** (3.589 Å) than in **6** and **7** (3.447 Å and 3.483 Å, respectively). Whether these are sterically ligand-imposed differences attributable to the shorter chelating arms in the ligands **2** and **3** compared to **1** or to a combination of steric and electronic differences due to the additional presence of Mn(III) ions in **6** and **7** is not clear.

The coordination around each Mn(II) ion is **5** is nearly octahedral with the angles ranging from 82.8° ($O_{acetate}$–Mn–$N_{pyridyl}$) to 100° ($N_{pyridyl}$–M–$N_{pyridyl}$). The widest angle is observed between two pyridyl groups as expected on steric grounds. The Mn(1)–$O_{phenoxy}$–Mn(2) angle of 115.8° is about the same as the angles in the mixed-valent complexes **6** and **7** (114.4 and 116°, respectively). These angles are significantly larger than the 99.9° angle observed in dimeric Mn(II) complexes bridged by two phenolate oxygens[13] but shorter than in triply acetate-bridged complexes.[14] This trend is to be expected due to the wider bite of the acetate ion bridge. The lengths and angles of bonds in **5** that are equivalent by the virtual C_2 axis are almost identical, showing the equivalence of the oxidation states of the two manganese ions. Distinctly different bond lengths and angles are observed for the two manganese ions in different oxidation states in the valence-trapped mixed-valent complexes **6**–**8**.[9a]

Complex **5** is colorless and shows no absorption in the visible region as expected for a high-spin Mn^{+2} complex. It shows two absorption peaks (280 and 300 nm) in the ultraviolet region due to the pyridyl groups of the ligand. The infrared absorption spectrum in the solid state shows peaks at 1590, 1560, and 1435 cm^{-1} assigned to and diagnostic of the bridging acetate groups.[15,9b] The molar conductivity in DMF confirms that **5** is a 1:1 electrolyte, supporting the formulation.

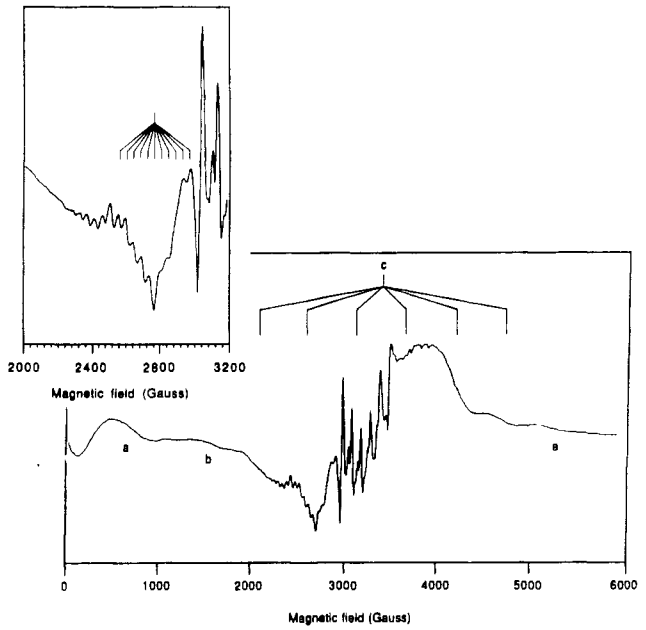

Figure 2. X-band EPR spectrum of $[Mn_2(LO)(\mu\text{-}OAc)_2(ClO_4)$ (**5**) (10^{-3} M) in DMF/CH_3OH glass at T = 77 K. Scan range = 0–6000 G; microwave frequency = 9.11 GHz; The inset shows the hyperfine structure due to isotropic coupling to the nuclei of two equivalent Mn(II) ions.

In the solid state, **5** has a room-temperature magnetic moment (corrected for ligand diamagnetic effects) of 5.2 μ_B, while in DMF solution, magnetic moments of 5.4 (298 K) and 5.5 μ_B (218 K) per manganese ion are observed. Similar values have been reported for the dimeric Mn(II) complex of bpeap[12a] in the solid state at room temperature and the acetate-bridged infinite chain Mn(II) complexes of the Robson type macrocyclic ligands at room temperature and down to 50 K.[9b]

The X-band EPR spectrum of **5** in the solid state is different from that in frozen solution. In the solid state, a spectrum with a six-peak fine structure and no hyperfine structure due to coupling to the manganese nuclei is observed. The spectrum of the frozen DMF/methanol solution glass at 77 K, shown in Figure 2, exhibits a hyperfine structure with features the same as those of a manganese semiquinone complex reported by Mathur and Dismukes,[16] and the transitions are similarly assigned. The peak near g = 2 with a six-line hyperfine structure (with a coupling constant of about 80 G) is attributed to a monomeric impurity which may arise from dissociation of the acetate bridging between the two manganese ions. This is superimposed on a six-peak fine structure labeled as c (Figure 2) centered near g = 2. On two of these peaks (the two lower field peaks), resolved 11-line hyperfine structures are observable (inset in Figure 2) with a hyperfine coupling constant of J = 43 G arising from coupling to the nuclei of two equivalent manganese ions (total nuclear spin I = 5). The hyperfine coupling constant of 43 G is close to half the hyperfine coupling constant exhibited by monomeric Mn(II) complexes and provides evidence that **5** contains a pair of Mn(II) ions that are magnetically equivalent and coupled with each other by an electron spin exchange interaction[16,17] consistent also with

(13) (a) Hodgson, D. S.; Schwartz, B. J.; Sorrell, T. N. *Inorg. Chem.* **1989**, *28*, 2226–2228. (b) Coucouvanis, D.; Greiwe, K.; Salifoglou, A.; Challen, P.; Simopoulos, A.; Kostikas, A. *Inorg. Chem.* **1988**, *27*, 593–594. (c) Kessissoglou, D. P.; Butler, W. M.; Pecoraro, V. L. *Inorg. Chem.* **1987**, *26*, 495–503.

(14) Wieghardt, K.; Bossek, U.; Nuber, B.; Weiss, J.; Bonvoisin, J.; Corbella, M.; Vitols, S. E.; Girerd, J. J. *J. Am. Chem. Soc.* **1988**, *110*, 7398–7411.

(15) (a) Deacon, G. B.; Phillips, R. J. *Coord. Chem. Rev.* **1980**, *33*, 227. (b) Weighart, K.; Bossek, U.; Ventur, D.; Weiss, J. J. *J. Chem. Soc., Chem. Commun.* **1987**, 347–349. (c) Mikuriya, M.; Torihara, N.; Okawa, H.; Kida, S. *Bull. Chem. Soc. Jpn.* **1981**, *54*, 1063–1067. (d) Sheats, J. E.; Czernuczewicz, R. C.; Dismukes, G. C.; Rheinhold, A.; Petrouleas, V.; Stubbe, J.; Armstrong, W. H.; Beer, R. H.; Lippard, S. J. *J. Am. Chem. Soc.* **1987**, *109*, 1435–1444.

(16) Mathur, P.; Dismukes, G. C. *J. Am. Chem. Soc.* **1983**, *105*, 7093–7098.

(17) Mathur, P.; Crowder, M.; Dismukes, G. C. *J. Am. Chem. Soc.* **1987**, *109*, 5227–5233.

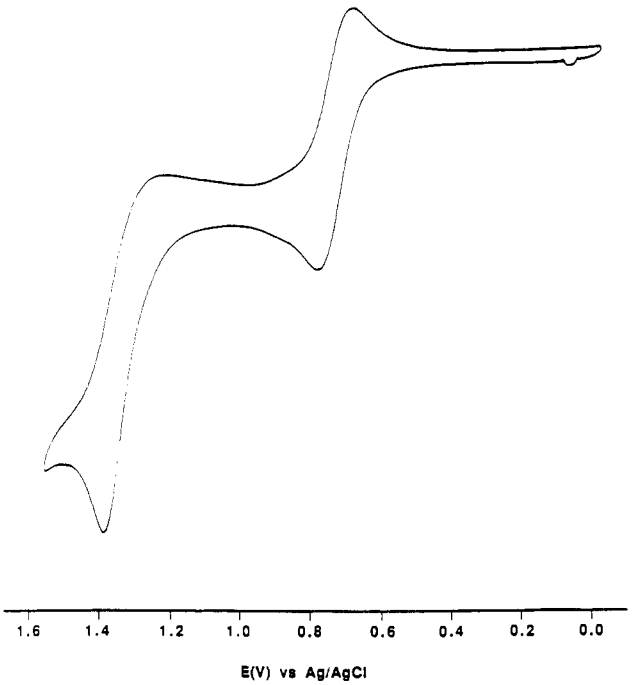

Figure 3. Cyclic voltammogram of **5**, $[Mn(LO)(\mu\text{-}OAc)_2](ClO_4)$, in acetonitrile, with 0.1 M $(n\text{-but})_4NPF_6$ supporting electrolyte and 100 mV/s scan rate using Ag/AgCl reference, glassy-carbon working, and platinum-wire auxiliary electrodes. A ΔE_p value of 80 mV is observed for the lower potential peak representing the quasi-reversible Mn^{II}_2/$Mn^{II}Mn^{III}$ redox process.

the 11-line hyperfine structure. The peak labeled b appears at half-field and is assignable to the $\Delta M_s = 2$ forbidden transition. The two peaks labeled as a in Figure 2 have been assigned, following the assignments by Mathur and Dismukes,[16] to be due to $\Delta M_s = \pm 1$ transitions to higher energy states. The similarity between the EPR spectra of **5** and the Mn(II) semiquinone complex reported by Mathur and Dismukes[16] confirms that the later has a dimeric structure as the authors have proposed based on the EPR spectrum.

The cyclic voltammetry of the solution of **5** in CH_3CN shows one quasi-reversible peak at 0.73 V and an irreversible peak at 1.28 V vs Ag/AgCl (Figure 3). These oxidation potentials are significantly higher than the potentials 0.47 and 0.435 V for the Mn^{II}_2/$Mn^{II}Mn^{III}$ redox process and 1.02 V for the $Mn^{II}Mn^{III}$/Mn^{III}_2 redox process reported in the cases of the analogous $Mn^{II}Mn^{III}$ complexes **6** and **7**, respectively.[8,18] The sizable difference in the redox potentials between complex **5** and the complexes **6** and **7** (approximately 0.25 V) arises from the difference between the ligands: the six-membered chelate rings formed by **1** and the five-membered chelate rings formed by **2** and **3** on complexation. A five-membered chelate ring stabilizes the higher oxidation state relative to a six-membered ring, hence the formation of the $Mn^{II}Mn^{III}$ complexes by the ligands **2** and **3** while **1** forms a stable Mn^{II}_2 complex with high oxidation potential. This variation in the redox potentials of the complexes of chelating ligands as a function of the chelate ring size (six- or five-membered chelate rings) is observed in other metal complexes of similar ligands also. For instance among copper complexes formed by tris(ethylpyridyl)amine (TEPA) and tris(methylpyridyl)amine (TMPA), a class of mononucleating tripodal ligands which present donor sets similar to **1** and **2** respectively, a difference of 0.56 V is observed in the redox potentials of $[Cu(TEPA)Cl]PF_6$ ($E_{1/2}$ = +0.17 V vs NHE) and $[Cu(TMPA)Cl]PF_6$ ($E_{1/2}$ = −0.39 V vs NHE)[19] showing the stabilization of the lower oxidation state (Cu(I)) by the six-membered chelate rings in the TEPA complex compared to the TMPA complex. In such copper complexes, each change from a five-membered to six-membered chelate ring among the complexes of the analogous tripodal ligands increases the oxidation potential of the Cu(I) complexes by about 0.2 V. A similar effect is observed in the copper complexes of the analogous thioether ligands.[20] In the present manganese complexes, we observe an increase in oxidation potential of an average of about 0.14 V per six-membered chelate ring formed.

The stability of **5** is also shown by the fact that it is isolated from the reaction of $Mn(ClO_4)_2 \cdot 6H_2O$ with ligand **1** in air whereas with ligand **2** or **3**, under the same conditions, the oxidized (mixed-valent) $Mn^{II}Mn^{III}$ complexes are isolated.[6,7] Also when an oxidizing agent such as aqueous hydrogen peroxide is added to a solution of **5** in methanol, first a brown solution forms but the solution then quickly fades in color and the starting complex is isolated unchanged, suggesting that very likely **5** is oxidized by hydrogen peroxide, but it reverts back to the stable Mn^{II}_2 complex **5**, probably by oxidizing the solvent.

Conclusion

We have synthesized and structurally and spectroscopically characterized a stable discrete dinuclear Mn^{II}_2 complex. The data reported add new information about discrete dinuclear manganese model complexes for the manganese enzymes. The EPR spectrum is consistent with the presence of two equivalent Mn^{2+} ions and confirms the proposed dinuclear structures for manganese complexes with similar EPR spectra. The high oxidation potentials exhibited by **5** in the cyclic voltammetry results and the unusual stability to oxidation shown by **5** demonstrate the dramatic effect of varying the chelate ring size from five in **6** and **7** to six in **5** on the redox properties of the manganese complexes.

Acknowledgment. We thank the National Institutes of Health (Y.G. and K.D.K.) and the NSF (J.Z.) for the support of this work. Y.G. thanks Dr. Zoltan Tyeklar (Chemistry Department, Johns Hopkins University) for his invaluable help in reviewing and preparing the manuscript.

Supplementary Material Available: Tables of atomic coordinates and equivalent isotropic displacement parameters, bond lengths, bond angles, anisotropic displacement parameters, and hydrogen atom coordinates (5 pages). Ordering information is given on any current masthead page.

(18) Suzuki, M.; Murata, S.; Uehara, A.; Kida, S. *Chem. Lett.* **1987**, 282–284. Hudson, A.; Kennedy, M. J. *Inorg. Nucl. Chem. Lett.* **1971**, *7*, 333.

(19) (a) Zubieta, J.; Karlin, K. D.; Hayes, J. C. *Copper Coordination Chemistry: Biochemical and Inorganic Perspectives*; Karlin, K. D., Zubieta, J., Eds.; Adenine Press: Albany, NY, 1983; pp 97–108. (b) Karlin, K. D.; Hayes, J. C.; Juen, S.; Hutchinson, J. P.; Zubieta, J. *Inorg. Chem.* **1982**, *21*, 4106–4108. (c) Patterson, G. S.; Holm, R. H. *Bioinorg. Chem.* **1975**, *4*, 257.

(20) Karlin, K. D.; Sherman, S. E. *Inorg. Chim. Acta* **1982**, *65*, L39–L40.